

**REDUCTION OF BACKSCATTERED
RADIATION FOR X-RAY IMAGE QUALITY
ENHANCEMENT**

by

ABDULLAH TAHER QAED NAJI

**Thesis submitted in fulfillment of the requirements
for the degree of
Doctor of Philosophy**

December 2016

DEDICATION

I would like to dedicate this work to my mother Na'ayem Saeed, and to my father Haji Taher Qaed, whose prayers have given me the strengths to complete this work.

ACKNOWLEDGMENT

First, all praise is for my creator ALLAH SWT the almighty for giving me the strength and courage to persevere throughout the duration of this research.

My great thanks to my Supervisor Professor Dr. Mohamad Suhaimi Jaafar for his support, ideas, creative comments, guidance, and his good leadership that guides me to the right methods. I also thank him for taking a lot of efforts to go through my research.

My grateful thanks go to all the academic staff in the School of Physics, Universiti Sains Malaysia, for their providing of modern studies.

My deep thanks to my father Haji Taher Qaed, and to my mother Na'ayem Saeed because their always encouragement and support throughout my life.

My gratitude goes to my wife Hanan Hassan, lovely son Refat Abdullah, and to my brothers and sisters for their patience along the period of my study

Also, I would like to thank every person who stood aside of me for the success of this work, and I would like to thank all my fellow colleagues and friends who have directly or indirectly participated in making this research possible, while it might be not possible to name them all here, their help is unforgettable forever.

TABLE OF CONTENTS

| | |
|---|------|
| ACKNOWLEDGMENT | ii |
| TABLE OF CONTENTS | iii |
| LIST OF FIGURES | ix |
| LIST OF TABLES | xiv |
| LIST OF SYMBOLS AND ABBREVIATIONS | xv |
| ABSTRAK | xvii |
| ABSTRACT | xix |
| | |
| CHAPTER 1 - INTRODUCTION | |
| 1.1 Background | 1 |
| 1.2 Problem Statement | 4 |
| 1.3 Research Objectives | 5 |
| 1.4 Scope of Research | 5 |
| 1.5 Research significance | 6 |
| 1.6 Outline of thesis | 6 |
| | |
| CHAPTER 2 - LITERATURE REVIEW | |
| 2.1 Introduction | 8 |
| 2.2 Factors affecting the X-ray emission spectrum | 8 |
| 2.3 X-ray interaction with matter | 9 |
| 2.3.1 Coherent scattering interaction | 9 |

| | | |
|--|--|----|
| 2.3.2 | The photoelectric effect interaction | 10 |
| 2.3.3 | Compton scattering interaction | 10 |
| 2.4 | Backscattered radiation | 12 |
| 2.5 | Effects of backscattered radiation | 13 |
| 2.6 | Previous studies on backscattered Radiation | 14 |
| 2.7 | X- ray Image quality | 19 |
| 2.7.1 | Image's contrast | 19 |
| 2.7.1(a) | Factors affecting on X-ray image's contrast | 22 |
| 2.7.1(b) | Optical Density | 23 |
| 2.7.1(c) | Optical density and light penetration through film | 23 |
| 2.7.1(d) | Image contrast indicator | 27 |
| 2.7.2 | Image's resolution | 27 |
| 2.7.2(a) | Image resolution indicator | 28 |
| 2.7.2(b) | Factors affecting on X-ray image's resolution | 29 |
| 2.8 | Previous studies on image quality | 30 |
| CHAPTER 3 - MATERIALS AND METHODS | | |
| 3.1 | Introduction | 34 |
| 3.2 | Materials and Instrumentations | 34 |
| 3.2.1 | X-ray Machine | 35 |
| 3.2.1(a) | X-ray Generator | 36 |
| 3.2.1(b) | X-ray tube | 36 |
| 3.2.1(c) | X-ray Control Panel | 37 |
| 3.2.1(d) | Cooling system | 38 |

| | |
|--|----|
| 3.2.1(e) Housing protective | 38 |
| 3.2.2 Mobile X-ray unit | 39 |
| 3.2.3 Dosimeters | 40 |
| 3.2.3(a) Ion Chamber Flat 30 cm ³ (Type 233612) | 40 |
| 3.2.3(b) Max 4000 Electrometer | 41 |
| 3.2.3(c) Ionization chamber (Type 77334) | 42 |
| 3.2.3(d) PTW UNIDOS Electrometer | 43 |
| 3.2.4 Holders | 44 |
| 3.2.5 Radiographic phantom | 44 |
| 3.2.6 RMI Aluminium step wedge | 45 |
| 3.2.7 Resolution test tool | 46 |
| 3.2.8 Cassette | 46 |
| 3.2.9 Radiographic film | 47 |
| 3.2.10 Automatic processing film machine | 47 |
| 3.2.11 Densitometer | 48 |
| 3.2.12 Anti – scatter grids | 49 |
| 3.3 Methods | 50 |
| 3.3.1 Fabrication of anti-scatter grids | 51 |
| 3.3.1(a) Grid's design | 51 |
| 3.3.1(b) Procedures of grid construction | 54 |
| 3.3.2 Experiments set up | 57 |
| 3.3.3 Quality control tests | 58 |
| 3.3.4 Dosimeters accuracy | 59 |
| 3.3.4(a) Dose determination for MAX 4000 electrometer | 59 |

| | | |
|-----------|--|----|
| 3.3.5 | Evaluation the capabilities of some materials in attenuation X-ray | 59 |
| 3.3.6 | Estimation backscattered radiation from some materials | 60 |
| 3.3.7 | Studying the effect of anti-scatter grid on total dose | 61 |
| 3.3.8 | Studying the effectiveness of anti-scattered grids on backscattered doses | 62 |
| 3.3.9 | Studying the effect of X-rays energy (kVp) on backscattered radiation dose | 62 |
| 3.3.10 | Studying the effect of ion chamber Position (backscattered angle) on recorded backscattered dose | 63 |
| 3.3.11 | Studying the effect of radiation intensity on backscattered radiation dose | 63 |
| 3.3.12 | Studying the effect of distance between X-ray source and surface of exposed object (SSD) on the backscattered dose | 63 |
| 3.3.13 | Evaluation of image's contrast | 64 |
| 3.3.13(a) | Estimating image's contrast | 64 |
| 3.3.14 | Evaluation of image's resolution | 65 |
| 3.3.14(a) | Estimating image's resolution | 66 |
| 3.3.15 | Safety and protection | 67 |
| 3.4 | Summary | 67 |

CHAPTER 4 - RESULTS AND DISCUSSION

| | | |
|----------|---|----|
| 4.1 | X-ray attenuation for some materials | 69 |
| 4.1.1 | X-ray attenuation using Lead shields | 69 |
| 4.1.1(a) | The effect of Lead thickness on reduction of X-ray dose | 70 |

| | | |
|----------|---|-----|
| 4.1.2 | X-ray attenuation by using copper shields | 72 |
| 4.1.2(a) | The effect of Copper thickness on reduction of X-ray dose | 73 |
| 4.1.3 | X-ray attenuation using Iron Steel shields | 74 |
| 4.1.3(a) | The effect of Iron thickness on reduction of X-ray dose | 75 |
| 4.1.4 | X-ray attenuation using Aluminium shields | 76 |
| 4.1.4(a) | The effect of Al thickness on reduction of X-ray dose | 78 |
| 4.1.5 | The effect of X-ray tube current and time of exposure (radiation exposure intensity) on the attenuation of X-ray by various metals. | 80 |
| 4.1.6 | X-ray attenuation using Concrete shields | 82 |
| 4.1.6(a) | The effect of cement shield thickness on atten. of X-ray | 84 |
| 4.1.7 | Backscattered radiation from some materials | 85 |
| 4.2 | Effect of fabricated anti- scatter grids on Backscattered radiation | 86 |
| 4.2.1 | Back scattered radiation dose with different X-ray units | 87 |
| 4.2.1(a) | X-ray machine type | 90 |
| 4.2.1(b) | The effect of anti-scatter grid on total dose | 93 |
| 4.2.2 | The effectiveness of anti-scatter grids at different (mAs) | 95 |
| 4.2.3 | Effect of dosimeter Position (back scatter angle) on recorded backscattered dose | 101 |
| 4.2.4 | Effect of X-ray field size on recorded backscattered dose | 103 |
| 4.2.5 | Effect of distance between X-ray source and imaged target's surface (SSD) on backscattered radiation doses | 105 |
| 4.3 | Effect of using anti-scatter grids on X-ray image quality | 107 |
| 4.3.1 | X-ray image contrast evaluation | 107 |
| 4.3.1(a) | Image contrast for different X-ray units | 108 |
| 4.3.1(b) | Image contrast variation at various X-rays energy (kVp) | 110 |
| 4.3.1(c) | Image contrast variation at various mAs | 114 |

| | |
|--|-----|
| 4.3.2 X-ray Image Resolution Evaluation | 116 |
| 4.3.2(a) Image Resolution for different X-ray units | 117 |
| 4.3.2(b) Image resolution variation at various kVp | 119 |
| 4.3.2(c) Image resolution variation at various mAs | 122 |
| 4.3.3 Summary of Findings | 124 |
| | |
| CHAPTER 5 – CONCLUSION, RECOMMENDATIONS AND FUTURE WORK | |
| 5.1 Conclusion | 127 |
| 5.2 Recommendations and Future Work | 128 |
| REFERENCES | 129 |
| | |
| APPENDICES | |
| Appendix A | 140 |
| Appendix B | 144 |
| Appendix C | 146 |
| Appendix D | 150 |
| Appendix E | 152 |
| | |
| LIST OF PUBLICATIONS | |

LIST OF FIGURES

| | | Page |
|-------------|--|-------------|
| Figure 2.1 | Coherent scatter interaction | 9 |
| Figure 2.2 | The photoelectric interaction | 10 |
| Figure 2.3 | Compton scattering occurs between moderate energy X-rays and outer-shell electrons | 11 |
| Figure 2.4 | Backscattered radiation | 13 |
| Figure 2.5 | Model defines X-ray image contrast | 21 |
| Figure 2.6 | Relationship between light penetration and film's optical density | 23 |
| Figure 2.7 | The Hurter and Driffield curve | 25 |
| Figure 2.8 | The effect of Scatter radiation on x-ray image contrast | 26 |
| Figure 3.1 | X-ray machine Toshiba model KXO-50S | 35 |
| Figure 3.2 | Basic X-ray tube components | 37 |
| Figure 3.3 | X-ray control panel | 38 |
| Figure 3.4 | Toshiba IME-100L X-ray machine | 39 |
| Figure 3.5 | Ionization chamber flat (PTW:233612) | 41 |
| Figure 3.6 | Electrometer (MAX 4000) | 42 |
| Figure 3.7 | Ionization chamber flat (PTW: 77334) | 42 |
| Figure 3.8 | PTW UNIDOS electrometer | 43 |
| Figure 3.9 | RMI radiographic phantom model 170B | 45 |
| Figure 3.10 | Aluminium steps wedge | 45 |

| | | |
|-------------|--|----|
| Figure 3.11 | Resolution test tool (PTW FREIBURG) | 46 |
| Figure 3.12 | Konica radiographic film cassettes | 47 |
| Figure 3.13 | Automatic processing film machine | 48 |
| Figure 3.14 | RMI Densitometer | 49 |
| Figure 3.15 | The fabricated anti-scatter grid | 50 |
| Figure 3.16 | Research methods schematic diagram | 51 |
| Figure 3.17 | The design of crossed grid | 53 |
| Figure 3.18 | Anti-scattered radiation grid design | 55 |
| Figure 3.19 | Grid's strips | 56 |
| Figure 3.20 | Geometrical designs of fabricated anti-scatter grids | 56 |
| Figure 3.21 | The position of Anti-backscatter grid during x-ray imaging | 57 |
| Figure 3.22 | The set up of experiments using fabricated grid | 58 |
| Figure 3.23 | Measurement of transmitting (penetrating) radiation | 60 |
| Figure 3.24 | Measurements of total dose | 61 |
| Figure 3.25 | Evaluation of image's contrast | 65 |
| Figure 3.26 | Evaluation of image's resolution | 66 |
| Figure 4.1 | Transmitting X-ray through 1 mm Lead Shield | 70 |
| Figure 4.2 | X-ray attenuation by Lead shields with different thicknesses | 72 |
| Figure 4.3 | Transmitting X-ray through 1 mm copper shield | 73 |
| Figure 4.4 | The effect of copper thickness on attenuation of X-ray | 74 |

| | | |
|-------------|--|----|
| Figure 4.5 | Transmitting X-ray through 1 mm iron steel shield | 75 |
| Figure 4.6 | The effect of Iron Steel thickness on attenuation of X-ray | 76 |
| Figure 4.7 | Transmitting X-ray through 1 mm Aluminium shield | 77 |
| Figure 4.8 | Penetrating x-ray doses through 1 mm shield of some metals | 78 |
| Figure 4.9 | The effect of Aluminium thickness on attenuation of incident X-ray | 79 |
| Figure 4.10 | Mass attenuation coefficient for different metals with 1 mm thickness | 80 |
| Figure 4.11 | X-ray attenuation percentages for several metals at different mAs | 82 |
| Figure 4.12 | Transmitting X-ray through concrete shields | 83 |
| Figure 4.13 | X-ray attenuation by cement shields with and without barium sulfate | 84 |
| Figure 4.14 | The effect of concrete thickness on attenuation of X-ray | 85 |
| Figure 4.15 | Backscattered radiation dose from several materials | 86 |
| Figure 4.16 | Backscattered radiation doses at different kVp for stationary X-ray unit | 87 |
| Figure 4.17 | The effectiveness of anti-scatter grids at different tube voltage | 89 |
| Figure 4.18 | Backscattered radiation doses for mobile X-ray unit | 91 |
| Figure 4.19 | The effectiveness of anti-scatter grids at different kVp | 92 |
| Figure 4.20 | Total dose of X-ray at different kVps | 94 |
| Figure 4.21 | Effectiveness of anti-scatter grids at different kVp | 95 |
| Figure 4.22 | Backscattered radiation dose at different radiation intensity | 96 |

| | | |
|-------------|---|-----|
| Figure 4.23 | Effect of anti-scatter grids at 50 kVp and different mAs | 96 |
| Figure 4.24 | Backscattered dose at different radiation intensities | 97 |
| Figure 4.25 | Effect of anti-scatter grids at 70 kVp and different mAs | 98 |
| Figure 4.26 | Backscattered dose at different intensities | 99 |
| Figure 4.27 | Effectiveness of grids at 90 kVp and different mAs | 99 |
| Figure 4.28 | Backscattered dose at 110 kVp and different mAs | 100 |
| Figure 4.29 | Effectiveness of grids at 110 kVp and different mAs | 101 |
| Figure 4.30 | Backscattered radiation dose at different backscatter angles | 102 |
| Figure 4.31 | Capability of grids in reducing photons with different backscattering angle | 103 |
| Figure 4.32 | Backscattered radiation dose at different field size | 104 |
| Figure 4.33 | The effectiveness of anti-scatter grids at different field size | 105 |
| Figure 4.34 | Backscattered radiation dose at different (SSD) | 106 |
| Figure 4.35 | Efectivness of anti-scatter grids at different SSD | 107 |
| Figure 4.36 | Image contrast indices for different X-ray units | 109 |
| Figure 4.37 | Contrast increasing percentage by using anti-scatter grids | 109 |
| Figure 4.38 | Image contrast indices at different X-ray tube voltages | 111 |
| Figure 4.39 | Increasing in contrast indices percentages at different kVps | 112 |
| Figure 4.40 | Increase of contrast indices by using different anti-scatter grids | 114 |
| Figure 4.41 | Image Contrast Indices at different mAs | 115 |

| | | |
|-------------|--|-----|
| Figure 4.42 | Contrast increasing percentage at different mAs | 116 |
| Figure 4.43 | Image Resolution Index (lp/mm) for different X-ray units | 118 |
| Figure 4.44 | Resolution index increasing percentages with different X-ray units | 119 |
| Figure 4.45 | Image resolution Index (lp/mm) with different kVp | 120 |
| Figure 4.46 | Resolution enhancement percentages with anti-scatter grids | 122 |
| Figure 4.47 | Image resolution index (lp/mm) at different mAs | 123 |
| Figure 4.48 | Resolution increasing percentages at different (mAs) | 124 |

LIST OF TABLES

| | | Page |
|-----------|---|-------------|
| Table 2.1 | Factors affecting the size and relative position of X-ray emission spectrum | 8 |
| Table 4.1 | Attenuated X-ray doses through 4 mm thickness of some metals | 81 |

LIST OF SYMBOLS AND ABBREVIATIONS

| | |
|-----------|---|
| θ | Backscattered angle |
| λ | Wavelength |
| Al | Aluminium |
| ALARA | As Low As Reasonably Achievable |
| B.S. Dose | Backscatter radiation Dose |
| BSDF | Backscatter Dose Factor |
| C | Coloumb |
| Ci | Curie |
| CI | Contrast Index |
| CT | Computed Tomography |
| DNA | Deoxyribo Nucleic Acid |
| DSA | Digital Subtraction Angiography |
| E | Electric Charge |
| E_k | Kinetic Energy |
| FDD | Focal spot to Detector Distance |
| FOV | Field of view |
| Gy | Gray |
| HVL | Half value layer |
| IAEA | International Atomic Energy Agency |
| ICRP | International Commission on Radiological Protection |
| in | Inch |
| kg | Kilogram |
| kVp | Kilovoltage peak |

| | |
|--------|--|
| lp/mm | Line Pairs/ millimeter |
| mA | Milliampere |
| mAs | Milliampere second |
| MC | Monte Carlo |
| MS 838 | Malaysian Standards code (Medical X-ray Diagnosis) |
| m | Meter |
| NCRP | National Council on Radiation Protection |
| NDT | Non Destructive Testing |
| OD | Optical Density |
| QC | Quality Control |
| R | Roentgen |
| Rad | Radiation absorbed dose |
| Rem | Roentgen equivalent in man |
| SEDR | Scan Equalization Digital Radiography |
| SSD | Source to surface distance |
| T | Time |
| TEDE | Total Effective Dose Equivalent |
| TLD | Thermo Luminescent Dosimeter |
| SOR | Scatter-to-Open field Ratio |
| Sv | Sievert |
| SPR | Scatter-to-Primary Ratio |
| V | Electric Potential Voltage |
| Z | Atomic Number |

PENGURANGAN SINARAN SERAKAN BALIK BAGI PENINGKATAN KUALITI IMEJ SINAR-X

ABSTRAK

Kajian ini umumnya untuk mengurangkan sinaran serakan-balik dalam sebuah bilik sinar-X. Ciri-ciri pengecilan sinar-X dalam beberapa bahan seperti plumbum, kuprum, besi keluli, aluminium dan konkrit telah dikaji di bawah beberapa parameter pendedahan yang berbeza untuk mengukur kebolehan bahan-bahan tersebut sinar-X tuju dan mengurangkan serakan-balik sinar-X. Plumbum dan ferum menghasilkan atenuasi yang baik untuk sinar-x tuju pada julat tenaga diagnosis radiografi (50-110 kVp). Manakala, ferum dan aluminium memantulkan sejumlah kecil dos sinaran serakan balik. Beberapa grid anti serakan-balik telah direkabentuk dan difabrikasi daripada besi keluli dan aluminium kerana lebih berkemampuan mengurangkan sinaran serakan-balik berbanding dengan bahan-bahan lain, terdapat keperluan untuk menjelaskan kemampuan mengurangkan grid yang difabrikasi dalam sinaran serakan balik dengan menggunakan pelbagai mesin sinar-X yang berbeza di bawah pendedahan yang berbeza (kVp, mAs). Maka, kajian ini menilai pengurangan serakan-balik menggunakan grid anti serakan balik. Kesan menggunakan grid anti serakan balik yang difabrikasi ke atas kualiti imej sinar-X juga dikaji dari aspek kontras dan resolusi imej. Grid besi keluli bersilang mempamerkan pengurangan sinaran serakan balik yang terbaik sehingga 49.24 % di bawah dedahan tenaga rendah (50 kVp). Keputusan juga menunjukkan bahawa kontras dan resolusi imej meningkat dengan cara mengurangkan sinaran serakan balik menggunakan grid anti serakan-balik yang telah difabrikasi. Peningkatan kontras dan resolusi imej adalah sehingga 36% dan 32%, masing-masing, dengan

menggunakan grid besi keluli bersilang. Oleh itu, keberkesanan grid anti serakan-balik yang difabrikasi dalam mengurangkan sinaran serakan balik adalah bergantung kepada bahan dan rekabentuk grid dan juga parameter dedahan sinaran.

REDUCTION OF BACKSCATTERED RADIATION FOR X-RAY IMAGE QUALITY ENHANCEMENT

ABSTRACT

This study mainly aims to reduce backscattered radiation inside an X-ray room. The characteristics of X-ray attenuation in several materials such as lead, copper, iron steel, aluminium, and concrete have been investigated under different exposure parameters to measure their abilities to attenuate incident X-ray and to reduce backscattered X-ray. Lead and Iron presented good attenuation values for incident X-ray at radiographic diagnosis energy range (50 -110 kVp), whereas iron and aluminium reflected the least amount of backscattered radiation dose. A number of anti-scatter grids have been designed and fabricated from iron steel and aluminium, because of their relatively better abilities to reduce backscattered radiation compared to other materials. There remains the need to elucidate the backscattered radiation reduction capabilities of fabricated grids utilizing different X-ray machines under different exposure sittings (kVp, mAs). Thus, this study evaluates the possibility of backscattered reduction using fabricated anti-scattered grids. The effect of using fabricated anti-scatter grids on X-ray image quality was also investigated in terms of image contrast and resolution. Crossed Iron steel grid exhibited the optimum backscattered radiation reduction of up to 49.24% under low energy exposure (50 kVp). The results also showed that image contrast and resolution increased by reducing backscattered radiation using fabricated anti-scatter grids. The image contrast and resolution enhancements increased up to 36% and 32%, respectively, with the use of crossed iron steel grid. Therefore, the effectiveness of fabricated anti-scatter grids in reducing backscattered radiation is

dependent on the grid's material and design, as well as the radiation exposure parameters.

CHAPTER 1

INTRODUCTION

1.1 Background

Radiography technology is applied in clinical diagnosis to produce medical x-ray image of the human body for the purpose of assisting physicians in accurately diagnosing illness and internal injuries. Hence, personnel working in an X-ray room deal with patients and sophisticated equipment to generate accurate representations of human anatomy and pathology (Dance et al., 2014). Radiography is a vital and frequently utilized diagnostic tool in medicine, and considered the most valuable imaging modality for examining bone fractures and other related abnormalities (Mohanta& Khanaa, 2013; Mittone, 2015). On the other hand, medical X-ray is one of the largest artificial sources of radiation exposure to patients, workers, and the general populace, hence there exists the problem of safely delivering radiation dose when imaging biological tissues (Foffa et al., 2009; Mittone, 2015).

For instance, the cell composition of human organs such as live-tissue are destroyed or damaged when exposed to sufficient dose of X-ray, whether primary (incident) or secondary (scattered) radiation. This change in cell is dependent on the level of exposure and cell's response, since cells are particularly susceptible to changes due to radiation during cell mitosis (Sinclair, 2012). Although most DNA damage is repaired immediately, a portion of a chromosome may be permanently altered i.e. mutation (Janssens et al., 2004).

The optimization of radiation dose and image quality in radiography has developed into an important field of research (Sun et al, 2012). The effective management of radiation exposure and radiological protection are vital rudiments of medical imaging quality (Vano et al., 2014). The task of diagnostic X-ray equipment

is to provide distinct and high quality images of high clinical value that can be used to effectively describe physical characteristics appropriate for every medical case. Hence, system parameters of the diagnostic tool needs to be optimized by manufacturers, so that radiologists can scan organs and systems under the best conditions with standard techniques (Schafer et al., 2012).

X-ray scatter is an intricate phenomenon that can cause significant degradation of image quality, mainly in terms of contrast, resolution and contribute to image noise. In addition it generates additional unwanted radiation dose to patients and personnel in an X-ray room (Yao& Leszczynski, 2008; Wu et al., 2009). The problem of scattered radiation exposure to medical personnel during radiological operation is imperative because of the position of the workers and patient in relation to the radiation source, and the long period of X-ray exposure. Hence, scattered radiation is considered the main source of the occupational radiation exposure (Naryshkin, 2007; Bushong, 2013). Therefore, there is a need to reduce backscattered radiation so as to protect patients and workers in an X-ray room from unnecessary radiation exposure (Nicholas, 2006).

To elucidate matter interactions with radiation from X-rays, the mechanism of X-ray propagation should be understood. When a beam of X-ray strikes any object or inner cladding of X-ray room, it is either scattered, absorbed, transmitted or reflected to backward (Holmes, 2013). Scattered photons are radiation that changes in direction due to interaction with some medium.

The scattered photons negatively affect radiographic image contrast thereby hindering accurate representations of human anatomy, and increase radiation dose that patients and medical personnel are exposed to (Denise, 2007).X-ray scatter is one of the foremost factors that negatively affect image quality by causing the under

estimation of attenuation coefficient in image reconstructions. The scattered radiation decreases image sharpness and contrast, which makes the image hazy and indistinct (Langmack, 2001; Katalin, 2012). The scattered radiation is initiated by Compton interaction, which occurs when an incident photon collides with an atomic electron to produce photons that lose energy because of the scattering interaction (Alzoubi et al., 2011).

The generated secondary photons continue to dissipate energy in different directions due to the scattering interactions (White, 2014). Scattered radiation can be categorized based on the direction of secondary photons, backscattered radiation consists of photons that collide with an object and reflect back at different backscattering angles, when the photons are reflected back with scattering angle greater than 90° (at various angles between 90° and 180°) with the incident photons, it is referred to as backscattered radiation, whereas side scattered radiation occurs when the photon scatters to the side or changed its trajectory by 90° from the initial photon beam direction (Mohamed, 2007).

Given the critical nature of scattered radiation as a fundamental limitation to X-ray image acquisition and the continuous grid attenuation of primary photons, the imaging dose needs to be increased in order to maintain the image quality (Zhu et al., 2009). Scattered X-rays induce redundant details on the radiographic image and produce a uniform optical density features on the screen-film combination, as well as generate uniform intensity in the digital image receptor, resulting in image contrast reduction (Bushong, 2013). When attenuated photons transmit through an exposed target and collide with patient's table or wall bucky, some of the backscattered photons reach the film screen or detectors, possibly affecting the imaging system and initiating the presence of redundant radiation dose in the X-ray room. Therefore,

scattered radiation photons (whether side scattered or backscattered) are constantly taken into consideration when producing a radiograph due to its effect on the image quality and exposure of medical personnel to the X-ray (Jaenisch et al., 2010; Neugschwandtner et al., 2015).

1.2 Problem statement

Radiography examinations are extensively applied in clinical diagnosis and considered a first line of investigation procedure for several cases. As a result, patients and medical personnel in the field of radiology are constantly exposed to backscattered radiation from the X-ray interactions, thereby increasing the risk of ionizing radiation. Another major problem is that the backscattered radiation can cause degradation of image quality. Imaging system with film screen combination require the enhancement of image quality in order to provide good quality particularly in area limited by advanced diagnostic systems such as digital radiography.

Radiographic anti-scatter grid is one of the most important methods to reduce scattered X-rays that reach the image's receptor (Kammel et al., 2010; Bushong, 2013; Schaepkens, 2015), but the major disadvantage that accompanies the use of radiographic anti-scatter grid is increased patient radiation dose (McFadden et al., 2013; Sabic et al., 2016). However, several researchers have shown interest in using beam catcher panel in reducing backscattered radiation (Abdul-Majid et al., 2005).

Therefore, this study attempts to provide the needed support to improve radiography and protect patients and operators from exposure to harmful radiation. This study will focus on x- ray imaging optimization to reduce the backscattered radiation in an X-ray room by using fabricated anti-backscatter grids and evaluate its

effectiveness on enhancement of image quality. The challenge of this study is to reduce backscattered radiation dose in an X-ray room by using fabricated anti-backscatter grids and to minimize radiation exposure during radiographic procedures without compromising image quality.

1.3 Research objectives

The main goal of this study is to reduce backscattered radiation for enhancement X-ray image quality by fabrication several anti-backscatter grids. A number of sub-objectives designed to achieve the main goal can be summarized as follows:

- a. To assess the capabilities of some materials, namely; lead, iron steel, copper, aluminium, and concrete in attenuating X-ray by measuring transmitted x-ray through its shields.
- b. To fabricate several anti-backscatter grids of various geometrical shapes from different materials.
- c. To compare the backscattered radiation dose in an X-ray room with and without the use of fabricated grids.
- d. To characterize the reduction in backscattered radiation of X-ray.
- e. To determine the contrast and resolution of X-ray image as well as the effectiveness of fabricated grids in enhancing X-ray image quality.

1.4 Scope of research

This research will focus on the fabrication of several anti-backscatter grids of various geometrical designs (crossed and linear) from some materials such as; Iron Steel, Copper, Aluminium, Lead, and Concrete to reduce the backscattered radiation in an X-ray room. Different types of general X-ray machines will be used as a source

for incident radiation, the exposures were carried out at different exposure parameters (kVp, mAs, field size, SSD). The backscattered radiation doses will be measured by using different dosimeters. The effect of backscattered radiation reduction on enhancement of X-ray image quality will be assessed by investigating the effectiveness of using fabricated anti-backscatter grids under film cassette on X-ray image quality. Radiographic image quality will be evaluated based on two indices: contrast index (using phantom steps wedge which allows an evaluation of image contrast), and resolution index (visual line pair per millimeter analysis lp/mm).

1.5 Research significance

The reduction of backscattered radiation inside X-ray room using fabricated anti-backscatter grids can improve radiation protection for patient and workers during diagnostic examinations as well as enhance X-ray image quality. The strategies proffered in this study describe the radiation attenuation behavior for some materials and introduce accurate method to measure backscattered radiation dose.

This study will offer a novel practical method to decrease backscattered radiation exposure for patients, staff, public, and image's receptor. The materials utilized in this work are economical, readily available and can easily be shaped and fabricated into different designs of anti-backscatter grids. In addition, this study will facilitate further research to extend the range of applications for reducing backscattered radiation dose in addition enhancing X-ray image quality.

1.6 Outline of thesis

This thesis consists of five chapters. Chapter 1 introduces the topic of the study and provides a brief description of backscattered radiation and its related hazards, problem statement, scope of research, research significance, and research

Objectives. Chapter 2 covers a concise review of related literature and theoretical aspects of backscattered radiation and image quality parameters. Chapter 3 describes the instruments and the performance of the methods employed in this research work. Chapter 3 also discusses the study methodology and procedures performed to achieve the necessary results. Chapter 4 reports the experimental results of this study, comprising the results of the comparative analysis of the X-ray attenuation of the selected materials as well as the results of efficiency of the fabricated anti-backscatter grids. The experimental results are discussed in Chapter 4. The thesis is concluded in Chapter 5, which provides a summary of major results, offers recommendations and suggests possible areas for future works.

CHAPTER 2

LITERATURE REVIEW

2.1 Introduction

X-ray is the most common radiation used in hospitals. This radiation is produced mainly by machines when high voltage electrons interact with matter to produce high energy radiation (Suryanarayana & Norton, 2013). X-ray is a type of energy similar to light and like gamma ray passes easily through fairly thick materials (Pelberg et al., 2011; Stanford, 2012). X-ray imaging system has three principal parts including the high voltage generator, the operating console, and the X-ray tube, which are designed to provide a large number of high kinetic energy electrons focused toward a small spot area on the anode. The primary function of X-ray imaging system is to accelerate electrons from the cathode to the anode in an X-ray tube to produce high energy photons (Bushong, 2013; Dance et al., 2014). Therefore, X-ray machines and the rooms they are used have built-in shielding, and the useful beam is restricted by a cone or an adjustable collimator (Palo, 2010).

2.2 Factors affecting the X-ray emission spectrum

There are a number of factors under the control of radiographers that influence the size and shape of the X-ray emission spectrum and therefore the quality and quantity of the X-ray beam. These factors are summarized in Table 2.1 (Bushong, 2013).

Table 2.1: Factors affecting the size and relative position of X-ray emission spectrum

| Factor | Effect |
|--------------------|---|
| X-ray tube current | Amplitude of spectrum |
| X-ray tube voltage | Amplitude and position |
| Added filtration | Amplitude; most effective at low energy |
| Target material | Amplitude of spectrum and position of line spectrum |
| Voltage waveform | Amplitude; most effective at high energy |

2.3 X-ray interaction with matter

X-rays (in the imaging energies range) interact with matter in different ways including coherent scattering, photoelectric effect, and Compton scattering, whereas pair production does not occur during X-ray imaging (Aichinger et al., 2011; Carlton & Adler, 2012).

2.3.1 Coherent scattering interaction

Coherent scattering (Rayleigh scattering) is a change in the direction of an incident X-ray without a loss of energy, coherent scattering interaction occurs with low energies diagnostic X-rays, approximately as used in mammography. In coherent scattering the incident photon interacts with and excites a target atom (Figure 2.1). The energy of incident photon causes oscillation for the electrons in the target atom in phase. Then the atom's electron cloud radiates this energy immediately, and emits a photon with energy equal to that of the incident photons, but in different direction (Bushberg et al., 2012; Dance et al., 2014).

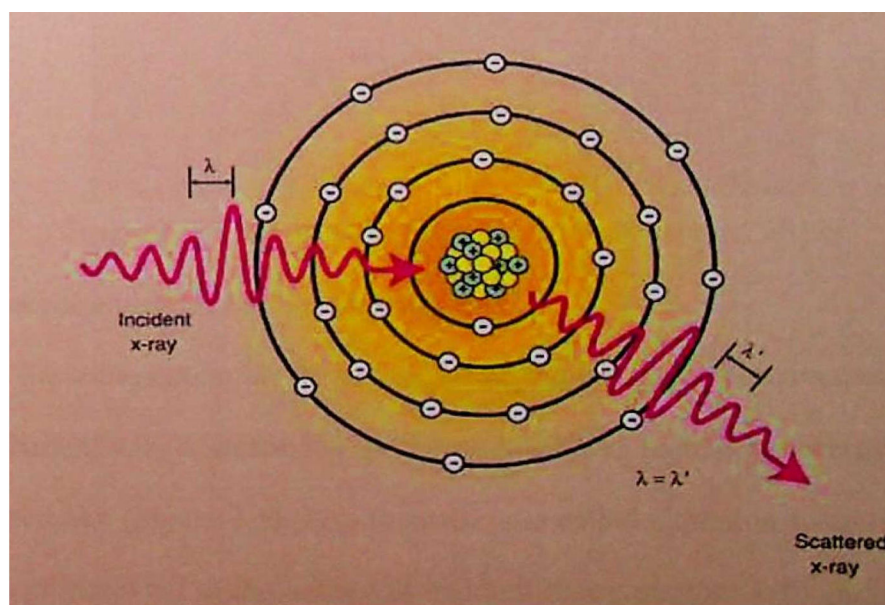


Figure 2.1: Coherent scatter interaction (Bushong, 2013)

2.3.2 The photoelectric effect interaction

During the photoelectric effect interaction, all of the incident photon energy is transferred to an ejected electron from the atom. The X-ray photons are not scattered, but they are totally absorbed (Figure 2.2). The incident photon's energy must be greater than or equal to the binding energy of the ejected electron (Carlton& Adler, 2012).The ejected electron from the atom which is called a photoelectron escapes with kinetic energy equal to the difference between the energy of the incident photon and the electron's binding energy. The probability of photoelectric effect is directly proportional to the atomic number and the density of absorber material (Bushberg et al., 2012; Bushong, 2013).

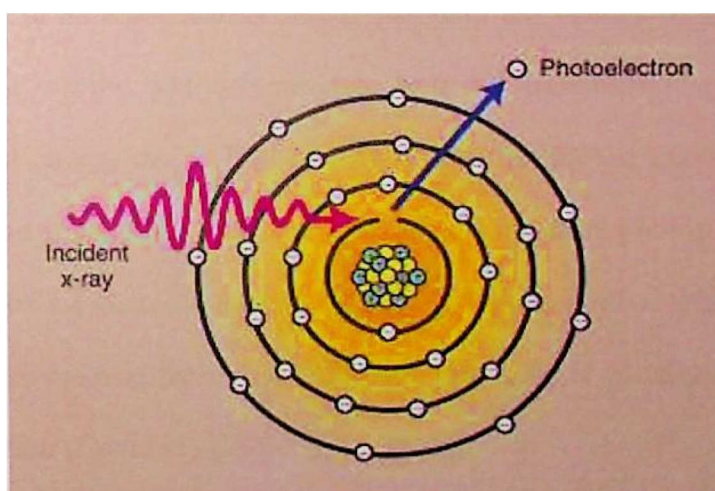


Figure 2.2: The photoelectric interaction (Bushong, 2013)

2.3.3 Compton scattering interaction

X-rays throughout the diagnostic range can undergo an interaction with outer-shell electrons, which scatter the X-ray photons and reduce its energy as well as ionizes the atom (Figure 2.3). This interaction is called Compton scattering which is inversely proportional to the energy of incident X-ray photon ($1/E$) and independent of the atomic number of absorber material (Aichinger et al., 2011; Bushong, 2013).

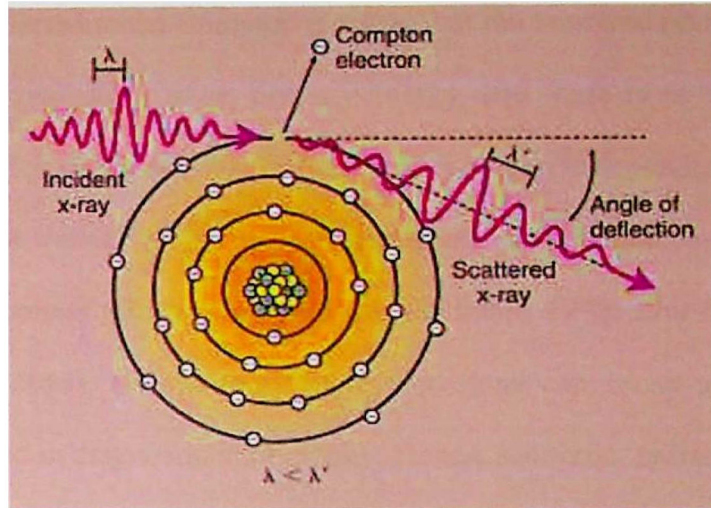


Figure 2.3: Compton scattering occurs between moderate energy X-rays and outer-shell electrons (Bushong, 2013).

Radiation scattering is a collision between a photon and an electron whose binding energy to an atom is very much less than the energy of the photon. In this collision, some of the photon's energy will be transferred to the electron if momentum and energy are to be converted; and the photon must be scattered, the scattered photon must have less energy than the incident photon (Johnson, 2016). The cross section for elastic scattering of hard X-rays in matter, which causes a phase shift of the wave passing through the object of interest, is usually much greater than that for absorption (David et al., 2007).

The energy of the scattered X-ray photon E' is given by Podgorsak (2010),

$$E' = \frac{E}{1 + E(1 - \cos\theta)/mc^2} \quad (2.1)$$

where; E is the energy of the incoming photon, m is the rest mass of the electron and C is the velocity of electromagnetic radiation (light), and the scattering angle, θ , can be in any direction. This is called the Klein-Nishina formula (Podgorsak, 2010). Therefore, Compton photons can be scattered in any direction, including 180° from the incident X-ray direction. As a deflection of 180° from the incident photons, more

energy is transferred to the Compton electron, but the scattered photon retains at least approximately two thirds of its primary energy, and there is no transferred energy with 0° deflection (Bushong, 2013). Scattered radiation is dependent on some factors such X-ray tube voltage (kVp), exposure intensity (mAs), field size, focal spot–table distance, and patient thickness (Marshall & Faulkner, 1992; Zhu & Bjarngard, 1994; Dance et al., 2014). Backscattered X-rays photons can cause a serious radiation exposure hazard in diagnostic radiography. Hence, scattered radiation is the source of most of the occupational radiation dose exposure that radiography’s staff receive (Theocharopoulos et al., 2014).

2.4 Backscattered radiation

Backscattered radiation is defined as a secondary radiation deflected with scattering angle more than 90° from the primary radiation (Farlex, 2012). Hence, backscattered photons refer to the part of scattered radiation that reflects back toward the source of radiation (Figure 2.4). The significant effect of backscattered radiation on image receptor and patient because of the short distance from the source of backscattered radiation such patient’s table, floor, standing bucky, and wall (Abdul-Majid et al., 2005; Stecker et al., 2009). In diagnostic radiography, backscattered radiation is responsible for the cassette-hinge image which sometimes seen on radiograph, even though the hinge is on the backside of the cassette (Aichinger et al., 2011). In such situations, the X-ray photons have backscattered from the wall of the room or the imaging table (Bushong, 2013).

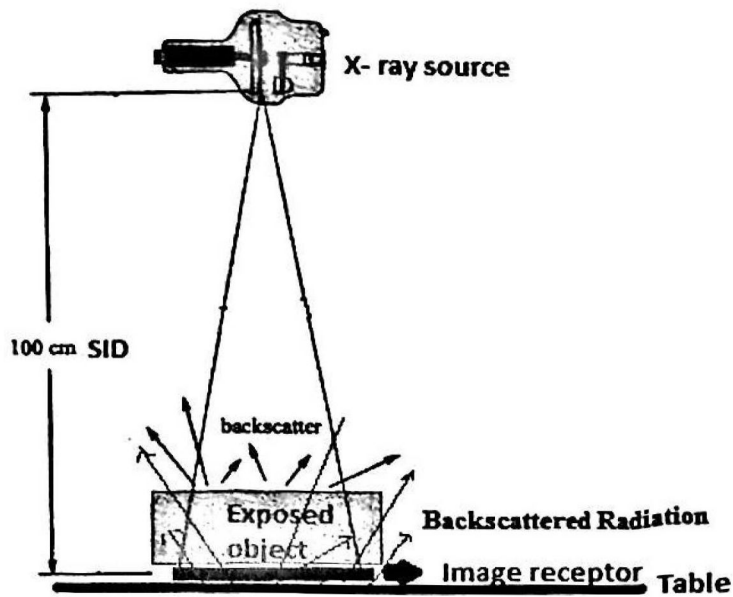


Figure 2.4: Backscattered radiation (Bushberg et al., 2012)

Therefore, backscattered radiation is an important portion of scattered radiation which can cause harm to the patients and workers in an X-ray room if their exposure exceeds the permissible value (Engel, 2006; Tsapaki et al., 2014). The reduction of backscattered radiation can be accomplished by appropriate selection of a material to line the walls on which the primary radiation is incident and by designing a beam catcher that is capable of absorbing significant portion of the scattered radiation (Abdul-Majid et al., 2005).

2.5 Effects of backscattered radiation

Backscattered radiation can have a significant effect on the quality of a radiograph, Backscattered radiation contributes with a large portion of scattered radiation which is the main source of exposure to radiation workers in an X-ray room. Therefore backscattered radiation protection for a patient and the technician inside the X-ray room during radiography, fluoroscopy, and interventional radiology procedures still require further optimization and investigation (Abdul-Majid et al., 2005; Theocharopoulos et al., 2014). On the other hand, scattered photons ends up at

a position on the image receptor during image acquisition convey no simple relationship to the position of the X-ray tube focus (Kitchen et al., 2014).

2.6 Previous studies

A number of studies have discussed backscattered radiation and investigated certain methods of backscattered radiation reduction. Eaton & Doolan (2013) reviewed backscattered measurements in kilo-voltage energies, where novel detectors and Gafchromic films were used to assess the reduction from underlying scattering material. The results showed that the use of lead shield could bring about large dose enhancement close to the lead interface, and a layer of 1 mm thick wax coating the lead shield was sufficient to remove lead radiation reduction effects for all kilo-voltage energies (40 kV to 300 kV). In a similar study, backscattered X-ray spectra of water surface was measured by Aoki and Koyama (2002) using a small silicon diode detector. The backscattered spectrums exhibited a narrower shape and lower mean energy compared to the primary spectrum. The ratio of the width of the backscattered spectrum to that of the primary spectrum was between 65% and 78%, while the ratio of the mean energy of the backscattered spectrum to that of the primary spectrum was between 83% and 94%.

Liu et al., (2000) studied the contribution of the backscattered radiation dose from collimator jaws using Monte Carlo simulations. The backscattered radiation dose contributed an estimated 3% of the monitor chamber's scored dose. Most of backscattered radiation dose are derived from the upper jaws (Y-jaws) of collimator because this part of the monitor chamber is closer to the radiation source than lower jaws (X-jaws). In addition, the results showed that photon output from backscattered radiation is directly proportional to field width.

In another study, Mainardi & Bonzi (2008) suggested an indirect method to measure backscattered X-ray radiation reflected from a carbon disk, which involves the use of eight detectors whose front windows are enclosed by metal sheets with different thicknesses. All detectors were placed on a plane perpendicular to the X-ray beam. Analytical equations were also derived to calculate the attenuation curves. The analytically calculated results were consistent with the MC simulated results, indicating the derived equations accurately describe the proposed detection approach.

The dose reduction from the loss of backscatter in superficial X-ray radiation therapy was studied by Healy et al., (2008). Ionization chamber measurements at the surface were performed in solid water with and without underlying lead. The dose perturbation was found at the lead surface beyond 3 cm depth compared to air, while the field size dependence of the dose perturbation was not strong. Differences of up to 3% were found between measured data for underlying lead and previous published results with different X-ray units. In another study, Butson et al., (2008) measured the dose reductions for superficial X-rays backscattered from bone interfaces to estimate the percentage dose changes at kilovoltage energies using ionization chamber and Gafchromic film. The bone does was affected on backscattered dose by reducing applied dose levels compared to water phantom measurements up to 12.5% of dose at zero depth.

Ravikumar et al., (2004) analyzed backscattered dose enhancements near different metallic interfaces which irradiated by high-energy X-ray therapeutic beams. PTW thin-window parallel-plate ionization chamber was used. The backscatter dose factor (BSDF) reached to the saturation value within few millimeters of all inhomogeneities. In addition, the saturation value was depended on the atomic number of the inhomogeneity. Furthermore, the range of backscattered

electrons from higher Z-inhomogeneity was higher compared to that from lower Z-materials. Moreover, the amount of backscattered secondary electrons, contributing to the increase in dose as the thickness of the inhomogeneity increased, particularly with lesser-energy photons (^{60}Co) compared to the higher energy photons.

Several studies have investigated factors that affect backscattered radiation. For instance, Huda (2004) examined the effect of the selection of kVp on dose and scattered radiation in computed tomography (CT) analyses. The results showed that a decline in the X-ray tube voltage from 120 to 80 kVp at a constant current (mAs) reduced the patient dose by approximately 60%. Even though the selection of kVp unaffected the amount of scatter-CT, as the thin detector (up to 2–3 cm) and the data acquisition geometry make sure that most scattered photons miss the detector, the contrast of a lesion in relation to the contiguous background increased with reduction in kVp. In a similar study, Jing et al., (1998) analyzed the effect of photon energy on scattered radiation in mammography using Monte Carlo simulations. The ratio of coherence to Compton scattered photons was found to decrease with the increase in photon energy. Furthermore, there scatter to primary ratio on the air gap was directly proportional to thickness of the Lucite phantom.

Similarly, Bootsma et al., (2011) investigated the effects of compensator and imaging geometry on the distribution of scattered X-ray in cone-beam CT (CBCT) using Monte Carlo model. Increasing the air gap, decreasing the cone angle, and the use of bowtie filtration were found to be effective approaches of minimizing scatter in CBCT, particularly the magnitude, and modifying the spatial distribution of the scattered photons. Berkhout et al., (2015) studied the specification of backscatter shield in order to provide good practice for utilizing handheld portable dental X-ray equipment. The study suggested that a lead shield should have a minimum thickness

of 0.25 mm or equivalent, with diameter of 15.2 cm, and should be positioned not beyond 1 cm from the end of the X-ray equipment.

Goren et al., (2014) assessed the backscatter radiation reduction capability of lead-filled acrylic shield which is attached to a portable X-ray tube. The doses were measured using water phantom and calibrated Thermo Luminescent Dosimeters (TLD). The backscatter measurements in front and behind the shield fall below the maximum acceptable radiation leakage according to the United States Food and Drug Administration regulations (100 mR/h) and also within the maximum permissible occupational dose. Abdul-Majid et al., (2005) demonstrated the possibility of reducing backscattered radiation up to approximately 30% and 45% using concrete catcher panel and iron catcher panel, respectively.

In a study on the rejection of scattered radiation in scan equalization digital radiography (SEDR) of lung and sub diaphragmatic regions, Liu and Shaw (2007) simulated Slot-scan and SEDR images for different slot widths. About 80% of scattered radiation was rejected by the anti-scatter grid in heavily attenuated regions, 70% in lightly attenuated regions and as high as 95% (with 1 cm slot width) without attenuation of the primary X-rays. Also, Watson et al., (2005) evaluated anti-scatter grid with diameter of 45 cm for gamma ray imaging. A very high grid ratio was designed using a modified version of Monte Carlo code to calculate radiation transport. The scatter rejection of the grid was estimated by comparing the ratio of direct and scattered radiation, the result of scatter rejection ratio was 30:1, compared with the theoretically possible scatter rejection ratio of 100:1. The lower measured ratios were attributed to background scatter of the back wall, ceiling, and floor. For image's contrast enhancement, the results demonstrated excellent contrast sensitivity for very thick objects.

The effect of using radiographic grid (anti-scattered grid positioned between the patient and image receptor) on patient dose has been evaluated. In a most recent study, Sabic et al. (2016) assessed the effect of radiographic grid on radiation dose in chest radiography for children. The patient exposure was determined by dose area product measurement. The results point out that patient's exposure dose was significantly reduced with the removal of anti-scatter grid. Also, McFadden et al. (2013) investigated the effect of removal of the anti-scatter grid on radiation dose. The dose reductions of 28% – 49% were achieved when the anti-scatter grid had been removed. In a similar study, Fritz & Jones (2014) determined patient thickness thresholds for radiographic grid use. Scatter-to-primary ratio was comparatively analyzed for thinner and adult patient. The results indicated that the scatter-to-primary ratio depend on field of view (FOV). Furthermore, the patient radiation dose was reduced by removing the anti-scatter grid for small patients.

It can be inferred from the reviewed studies that the use of radiographic anti-scattered radiation grid between the patient and image receptor can reduce the effect of scattered radiation on image receptor; however the main disadvantage associated with the use of radiographic grid is the increased patient radiation dose. Thus, there is the need for further studies to discover other methods capable of improving image quality without increasing patient radiation dose. This study suggests the fabrication of different types of anti-scatter grids from low-cost materials that can be easily shaped into different designs to reduce backscattered radiation and improve radiation protection inside the X-ray room.

2.7 X-ray image quality

X-ray image quality could be expressed by the exactness of representation of the anatomical structure on medical X-ray image (Guy and Flytche, 2005). X-ray image quality is not a single factor but can be described with characteristics such as resolution, contrast, beam alignment, and collimation alignment, although the beam alignment and the collimation alignment are only related to the quality of X-ray tube, and are not dependent to the X-ray parameters (Hobbie & Roth, 2007; Sezdi, 2011). Therefore, X-ray images are assessed by three quantities: the image's contrast, the degree of unsharpness (image's spatial resolution), and the patient dose (Fauber, 2016).

2.7.1 Image's contrast

Image contrast is one of the most important characteristics of X-ray image quality. Contrast arises from the areas of light, dark, and shades of gray on the X-ray image, these variations make up the radiographic image (Bushong, 2013). Contrast could be expressed by the degree of difference in optical density between adjacent areas of a radiograph or by the intensity difference in adjacent objects or regions of the image. The contrast expresses these differences as recorded on the radiograph (Carlton& Adler, 2012).

X-ray image contrast is a combination of two types of contrast subject's contrast, and image receptor's contrast. The subject's contrast refers to the contrast produced due to the differences in anatomical structures under examination, and expresses these differences in the number of X-ray photons emerging from adjacent regions of the patient being scanned. The subject's contrast depends on the differences in atomic number, density, thickness, and the energy spectrum of the X-

ray beam emitted by the source (Prakash et al., 2011). Whereas the image receptor's contrast refers to the contrast produced as a result of the X-ray image's receptor being employed. Also, image receptor's contrast refers to the ability of the image's receptor to convert the differences in photon intensity across the X-ray beam into the differences in film's optical density (Yumpu, 2015). For high contrast radiograph, individual objects stand out and their edges are clearly defined. Whereas for low contrast radiograph, the individual objects lose some of their clarity, and their edges be softened or blurred (Guy & Flytche, 2005; Suetens, 2009; Carver et al., 2012; Bushong, 2013).

According to Figure 2.5, the intensity at the middle of target object to be I_1 , and a reference point in the image just outside the object in the background to be I_2 . Then the contrast, C , is defined to be:

$$C = \frac{I_1 - I_2}{I_2} \quad (2.2) \quad (\text{Guy \& Flytche, 2005})$$

X-ray photons which produced by Compton scatter can produce noise and reduce image contrast, it makes the image less visible. With scattered photons, the contrast is decreased and the edges of the profile are softened as shown in Figure 2.6 (Guy & Flytche, 2005; Bushong, 2013).

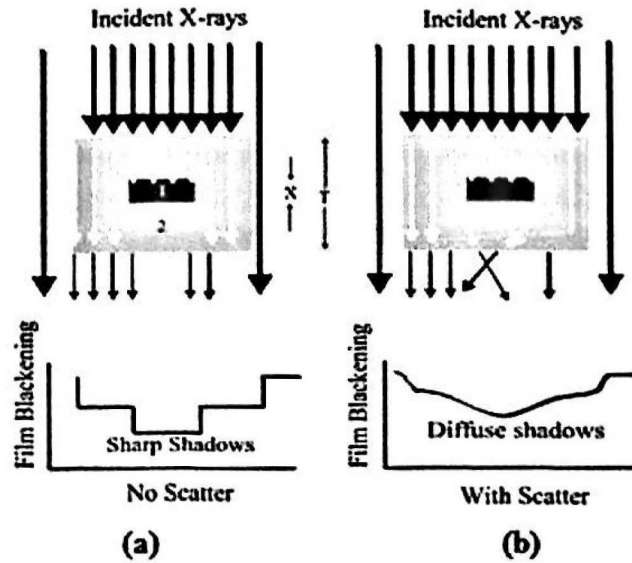


Figure 2.5: Model defines the X-ray image contrast and shows the effect of scatter radiation on image contrast. (a) No scatter radiation, the production image has sharp shadows and more contrast. (b) With scatter radiation, the image contrast decreases to the extent that the edges of the image details become softened (Guy & Flytche, 2005).

This definition can be used to estimate the differences in attenuation of objects in a radiographic image. For each the intensities (I_1 , and I_2), the contrast expression consists of two terms, the primary X-rays is termed as P , and the scattered X-rays which termed as S , both types of X-rays reach the detector. Thus, the intensities can be written as follows:

$$I_1 = P_1 + S_1 \quad (2.3)$$

$$I_2 = P_2 + S_2 \quad (2.4)$$

$$\text{With assumption: } S_1 \cong S_2 \cong S \quad (2.5)$$

The scatter can be considered to add a background haze, S , to both radiation intensities. It is assumed that the scatter contribution is the same to both regions.

Therefore, the contrast is reduced to

$$C = \frac{P_1 - P_2}{P_2 + S} \quad (2.6)$$

Scattered radiation can greatly reduce X-ray image contrast to the extent that subtle opacities may not be visualized (Guy & Flytche, 2005; Yumpu, 2015). Primary X-ray photons form a useful radiograph with perfectly sharp shadows. On the other hand, scattered photons arise from any exposed region and ends up at a position on the image receptor during image acquisition. These scattered photons convey no simple relationship to the position of the X-ray tube focus (Kitchenet al., 2014). Therefore, the ideal radiograph is degraded in sharpness by these scattered photons because the scattered component of the transmitted radiation does not possess the simple straight-line relationship between X-ray tube focus, patient point, and image point. Hence scattered photons modify the resulting intensity at the particular point in the image (Guy & Flytche, 2005; Fleckenstein & Trantum, 2014).

2.7.1 (a) Factors affecting on X-ray image's contrast

Image contrast is affected by some factors which mainly contribute to increase scattered radiation namely; increased kVp, increased X-ray field size, and increased patient thickness or exposed area (Bushong, 2013). Scattered radiation reduction can be achieved by decreasing the energy of incident radiation (kVp) and thereby increasing the patient's radiation dose because of the increased photoelectric absorption (Bloomfield et al., 2015). An important method for forward scattered radiation (which scatters within the patient) reduction can be obtained by utilizing a radiographic grid (anti-scatter grid). The available anti-scatter grid consists of thin strips of lead or high atomic number material, packed together with interspaces

between them from low atomic number material. This grid is placed between the patient and image receptor (Podgorsak, 2010).

2.7.1 (b) Optical Density

An X-ray film is a negative recorder, which means that increased X-ray photons exposure causes the developed film to become darker (opposite the case of photographic film, more light photons exposure produces brighter response). The degree of darkness of the film is quantified by the optical density (OD), which is measured with a densitometer (Whaites & Drage, 2013; Fleckenstein & Trantum, 2014). The densitometer is a simple device that shines white light onto one side of the developed film and electronically measures the amount of light reaching the other side. The measurements of OD correspond to that specific area of the film (Heindel, 2011; Carver et al., 2012).

2.7.2 (c) Optical density and light penetration through radiographic film

The optical density of film is assigned numerical values related to the amount of light that penetrates the film (Hendee & Ritenour, 2003; Dundar et al, 2010). Increasing film density decreases light penetration (Figure 2.6).

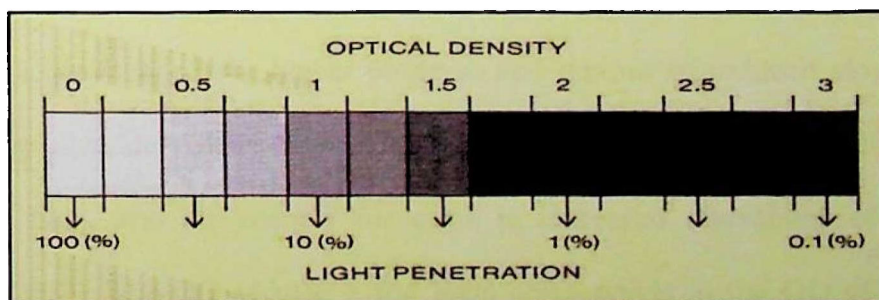


Figure 2.6: Relationship between light penetration and film optical density (Sprawls, 2015).

The relationship between density values and light penetration is exponential (Figure 2.7). If the intensity of the light measured with no film in the densitometer is

given by I_0 , and the intensity measured at a particular location on a film is given by I , then the transmittance (T) of the film at that location and the OD are defined as follows:

$$T = \frac{I}{I_0} \quad (2.7)$$

And the
$$OD = -\log_{10} T = \log_{10} \frac{1}{T} = \log_{10} \frac{I_0}{I} \quad (2.8)$$

Optical density can be defined as the logarithmic measure of the ratio of transmitted light to the incident light through the film image (Dundar et al., 2010)

So the inverse relationship is
$$T = 10^{-OD} \quad (2.9)$$

A Hurter and Driffield (H &D) curve is a description of a film's optical density as a function of the log of radiation exposure. The H & D curve consists of some regions including; the shoulder, the linear region, and the toe. At intermediate radiation exposure levels, small changes in exposure cause large changes in OD. This intermediate region called the straight-line portion, the region in which a properly exposed radiograph appears (Bushberg et al., 2012; Tsalafoutas et al., 2014).

The contrast of a radiographic film is related to the slope of the H & D curve; regions of higher slope have higher contrast, and regions of reduced slope (i.e., the toe and the shoulder) have lower contrast. When radiographic contrast is low, latitude is high, and the margin for error is increased (Bushberg et al., 2012; Bushong, 2013). The OD of base + fog level corresponds to the OD of unexposed film as it is illustrated in Figure 2.7.